Journal of Physics:
Conference Series



**PAPER** • **OPEN ACCESS**

# Fracture Properties and Applications of Freestanding Thin $Ti_3C_2T_x$ MXene Structures

To cite this article: A Kamal *et al* 2025 *J. Phys.: Conf. Ser.* **3058** 012010

# Fracture Properties and Applications of Freestanding Thin $Ti_3C_2T_x$ MXene Structures

**A Kamal[1,2,4], B Li[2,3], L Zheng[1,2], and K Liao[2,3]**

[1] Department of Mechanical and Nuclear Engineering, Khalifa University of Science and Technology, 127788, Abu Dhabi, UAE.
[2] Research & Innovation Center for Graphene and 2D Materials (RIC-2D), 127788, Abu Dhabi, 9 United Arab Emirates.
[3] Department of Aerospace Engineering, Khalifa University of Science and Technology, 127788, Abu Dhabi, UAE.
[4] Production Engineering and Mechanical Design Department, Faculty of Engineering, Tanta University, Egypt.
E-mail: kin.liao@ku.ac.ae

**Abstract.** Two-dimensional (2D) materials are unique nanomaterials that have a sheet-like structure with a high surface area and nanoscale thickness. These prominent materials are characterized by their outstanding electrical, chemical, optical, and mechanical properties. Accordingly, they represent typical solutions to revolutionize various technologies. Transition metal carbides, nitrides, and carbonitride (MXenes) are a novel family of 2D materials that hold significant potential for future applications. Processing MXenes into freestanding thin films or 3D structures is desirable to convey their intrinsic properties on a macroscopic scale. Such structures feature densely packed, hierarchically organized assemblies of pristine nanosheets. This study focuses on exploring the different properties of $Ti_3C_2T_x$ MXene thin films, including their mechanical properties and fracture toughness. The fracture behavior of $Ti_3C_2T_x$ MXene strips without cracks and in the presence of sided cracks, at varying strain rates, was investigated. Additionally, their electrical conductivity and electromagnetic interference (EMI) shielding capabilities were evaluated. The results reveal that sided cracks deteriorate the mechanical integrity of the $Ti_3C_2T_x$ MXene films. Furthermore, these films exhibit dependency on the applied strain rate. Thus, the fracture toughness ($K_{IC}$) dropped from 1.77±0.008 MPa.m$^{0.5}$ to 1.37±0.15 MPa.m$^{0.5}$ for films loaded at strain rates of 0.1 and 0.001 min$^{-1}$, respectively. The higher the strain rate, the higher the tensile strength and fracture toughness. Additionally, the $Ti_3C_2T_x$ MXene films achieved an electrical conductivity of 2300 S.cm$^{-1}$ and a total electromagnetic interference effectiveness of 44±2.7 dB with a considerable level of absorption.

## 1. Introduction

Recently, 2D materials such as graphene, MXenes, and hexagonal boron nitride (hBN) have been recognized for their large lateral size, flexibility, and mechanical rigidity [1]. For example, a monolayer of graphene and $Ti_3C_2T_x$ MXene exhibits Young's modulus ($E$) of 1 TPa and 0.484 TPa, respectively [2,3]. Along with these exceptional features, they demonstrate superior tunability for tailorable mechanical properties [4]. Accordingly, they have found tremendous usage for several electronic applications [5]. This warrants studying their deformation and fracture properties either in a freestanding form or as a reinforcement for a composite material.

Incorporation of 2D materials as nanofillers, thin coatings, or freestanding films in various applications is imperative for exploring their mechanical and fracture properties under various loading conditions. Thus, investigating their properties is of interest to estimate their performance, lifetime, and failure mechanisms. It was demonstrated in various studies that the mechanical properties and fracture toughness of 2D materials-based nanocomposites are much higher than those without 2D materials, even at lower concentration values [6]. These improvements are accompanied by enhanced performance in various applications, such as hydrogen barrier [7], and strain and temperature sensors [8].

Thin films made of pristine 2D materials such as graphene [9], graphene oxide (GO) [10], and MXene [11] show outstanding mechanical properties. For instance, a few micrometers thick $Ti_3C_2T_x$ MXene films, fabricated via vacuum-assisted filtration (VAF) technique, showed remarkable mechanical properties that accomplish a tensile strength of 85 MPa [12]. However, Kamal et al. [13] revealed that the mechanical properties of thin films constructed of 2D materials have a high dependency on several parameters, such as fabrication techniques, flake size, post-processing, and the test conditions. This sensitivity is mainly related to the variation in the interlayer characteristics, such as water content and functional groups [14]. Fabrication of $Ti_3C_2T_x$ MXene films via the blade coating approach provides precise controllability of the flakes' alignment. The high scalability of such technique is coupled with achieving superior tensile strength that peaked up to ≈570 MPa [15]. Moreover, controlling the $Ti_3C_2T_x$ MXene flake's lateral size can produce ultra strong films with high packing densities that yield a tensile strength of 739 MPa [16]. Moreover, Vinod et al. [17] demonstrated that the deformation behavior of GO films is sensitive to the applied strain. It was proven that decreasing the strain rate prompts the transition of the deformation from brittle to ductile. Fracture toughness of freestanding thin films (20μm thick) made of GO and hybrid GO/MWCNT has been studied under both opening mode (I) and tearing mode (III) loading [18]. The results demonstrated that the size of nanosheets has a considerable impact on the strain energy release rate at different crack lengths, since the films made of large GO nanosheets had enhanced strain energy release rates compared to those made of small nanosheets. Additionally, intercalating a low amount of MWCNT (5 wt.%) has improved the fracture properties of the hybrid film.

MXenes are recognized for their extraordinary electrical conductivity, which can achieve 11000 $S.cm^{-1}$ [19]. Their flexibility, mechanical stiffness, electrical conductivity, and adaptable processing in the form of thin films and coatings offer high potential to be utilized in EMI shielding applications. Pristine $Ti_3C_2T_x$ MXene, its hybrids, and composites are appropriate materials to protect electronic devices against electromagnetic waves (EMWs) [20]. For instance, Shahzad et al. [21] showed that $Ti_3C_2T_x$ MXene films with a thickness of 45μm have an EMI shielding effectiveness of 92 dB, which is comparable with metals. $Ti_3C_2T_x$ MXene/Wood Pulp Fabric attained a superb EMI shielding capabilities of about 90.2 dB [22]. Li et al. [23] showed that heterogeneous films composed of $Ti_3C_2T_x$ MXene and carbon nanosheets have a remarkable EMI shielding performance of 52.8 dB. This work aims to investigate the various properties of $Ti_3C_2T_x$ MXene thin films, including their mechanical properties and fracture toughness, at varying strain rates from 0.1 to 0.001 $min^{-1}$. Additionally, the electrical conductivity and EMI shielding capabilities of such films were evaluated.

## 2. Experimental

### *2.1. Material*

$Ti_3AlC_2$ powder with a particle size ≤ 40 μm was procured from Carbon-Ukraine, Ltd (Ukraine). Lithium fluoride (LiF) powder and hydrochloric acid (HCl, 37%) were obtained from Sigma-Aldrich, Germany.

### *2.2. Fabrication of MXene films*

$Ti_3C_2T_x$ MXene was synthesized following the minimal intensive layer delamination (MILD) approach. In this technique, the Al layers within the parent $Ti_3AlC_2$ MAX phase powder are etched via *in situ* HF etchant that is formed by the interaction of LiF (1.6 gm) with (15mL of 9 M) HCl acid [24]. The etching process lasts for 24 h under stirring at 40°C. Finally, the obtained solution is washed with deionized (DI)

water via centrifugation at 3500 rpm until reaching pH ≈ 6 to collect the $Ti_3C_2T_x$ MXene, as shown in Figure 1a. After that, the obtained $Ti_3C_2T_x$ MXene suspension with a concentration of (5 mg/mL) was used to fabricate a thin film with controlled thickness via a vacuum-assisted filtration (VAF) process [25], as shown in Figure 1b. The film's thickness was adjusted to 18µm by controlling the solution's amount and concentration. It is obvious that the fabricated film is flexible, as presented in Figure 1c.

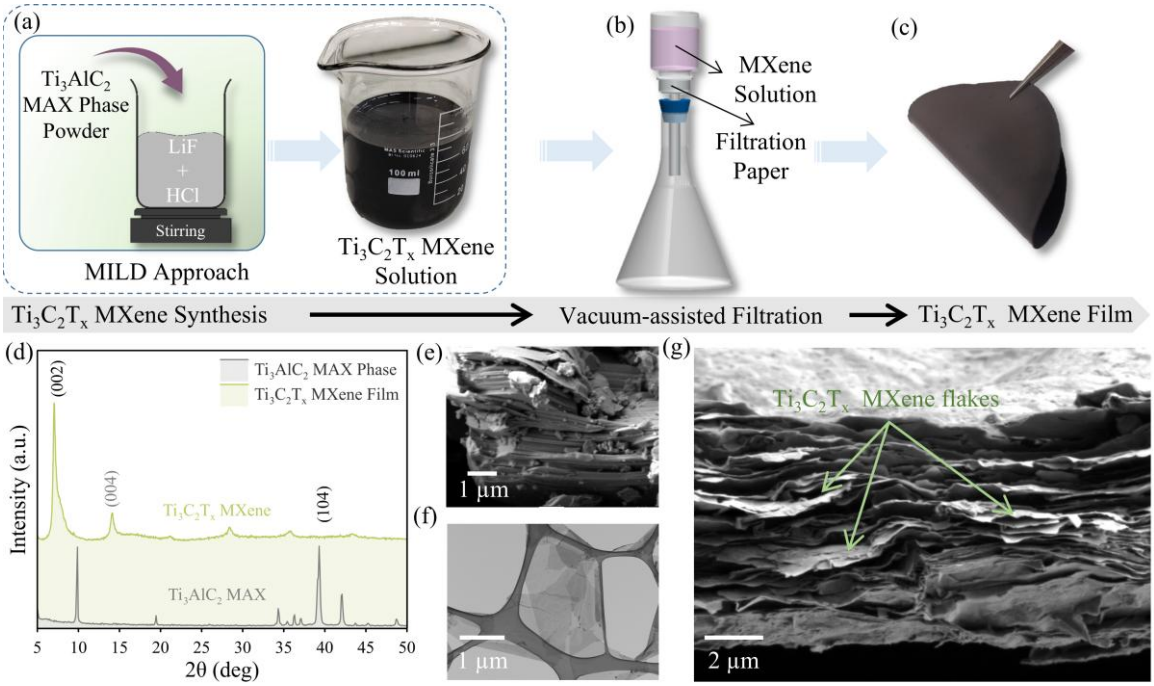


**Figure 1.** (a) Synthesis approach of $Ti_3C_2T_x$ MXene solution. (b) Fabrication of $Ti_3C_2T_x$ MXene film via vacuum-assisted filtration (VAF) process. (c) As-fabricated $Ti_3C_2T_x$ MXene film. (d) XRD patterns of MAX phase ($Ti_3AlC_2$) powder and the fabricated $Ti_3C_2T_x$ MXene film. SEM images of (e) MAX phase ($Ti_3AlC_2$) powder, (f) the $Ti_3C_2T_x$ MXene monolayer, and (g) the cross-section of the $Ti_3C_2T_x$ MXene film.

### *2.3. Characterization*

X-ray diffraction (XRD) was performed on a Brucker D2 phaser XRD diffractometer, using voltage and current of 30 KV and 10 mA, respectively. A field-emission scanning electron microscope (FE-SEM) (Joel 7610, Japan) was utilized to examine the surface morphology and the acquired fracture surface of $Ti_3C_2T_x$ MXene films. The successful exfoliation of $Ti_3C_2T_x$ MXene flakes with a uniform nanostructure and a flat morphology was confirmed by using a Tecnai transmission electron microscopy (TEM) 200 kV machine. The uniaxial tensile and fracture toughness tests were conducted via an Instron 5948 universal testing machine (UTM) at room temperature (RT). Longitudinal rectangular $Ti_3C_2T_x$ MXene strips with 8 mm width, 25 mm length, and 17±1.5 µm thickness were fixed on the UTM using soft tensile grippers and then loaded at a constant strain rate. The tensile strength, failure strain, and fracture toughness were determined by the average of five test results. A vector network analyzer (Agilent, E5071CENA) with a rectangular waveguide (WR-90) was used for measuring EMI shielding. The electrical conductivity of the obtained films was measured via an Ossila Four-Point Probe System (MCP-T610 model, Mitsubishi Chemical, Japan).

## 3. Results and Discussion

MXenes represent typical substances that combine a wide range of properties. Accordingly, they offer a vital performance for various applications. Assembling such materials in the form of free-standing thin

films introduces a great chance to investigate their performance on a macroscopic scale. In this work, the effective preparation of $Ti_3C_2T_x$ MXene was confirmed by monitoring the change taking place in the XRD patterns. As shown in Figure 1d, pure $Ti_3C_2T_x$ MXene was synthesized. Additionally, the SEM image (Figure 1e) of the $Ti_3AlC_2$ MAX phase shows its layered structure. After etching, transparent $Ti_3C_2T_x$ MXene sheets with considerable lateral size were acquired, as shown in Figure 1f. SEM image of the obtained $Ti_3C_2T_x$ MXene films shows a homogenous and compacted structure, as presented in Figure 1g. Investigating the robustness, mechanical performance, and fracture properties of such materials and the various properties of such films is essential for real-time applications.

### *3.1. Mechanical Properties*

The mechanical properties of $Ti_3C_2T_x$ MXene films under uniaxial tensile loading were investigated. The unique structure of such films that are composed of overlapped nanoflakes can offer relative sliding between the adjacent flakes. To highlight this behavior, the $Ti_3C_2T_x$ MXene films were tested under various strain rate levels, which are 0.1, 0.01, and 0.001 $min^{-1}$. As shown in Figure 2b, the obtained mechanical properties show sensitivity toward the applied strain rate. The higher the strain rate, the higher the tensile strength and the lower the failure strain. Loading the specimen under a strain rate of 0.1 $min^{-1}$ achieved a tensile strength of 17.2±0.6 MPa compared to 11.6±0.6 MPa for those tested under 0.001 $min^{-1}$. This behavior shows that the interactions and the relative sliding between the neighboring flakes play a crucial role in stress transfer due to the surface-rich functional groups. Accordingly, they control the overall mechanical properties. In this first stage of the loading, the straightening of individual wrinkled flakes is the dominant deformation mechanism, followed by relative sliding and straining of the individual flakes. Finally, the existing voids motivate the initiation of cracks that propagate rapidly until failure. Examination of the fracture surface revealed that pulling out of the $Ti_3C_2T_x$ MXene flakes is obvious, as shown in Figure 1g. Consistent observation was noted for GO films in previous investigations [17].

### *3.2. Fracture Toughness*

For a profound understanding of the fracture deformation of $Ti_3C_2T_x$ MXene films, investigating their fracture toughness in the presence of sided cracks is of interest. Thus, $Ti_3C_2T_x$ MXene specimens with double-edge notched tension (DENT) geometry (Figure 2a) were used to evaluate the fracture toughness under various strain rates. A sharp razor blade was used to introduce identical two-sided cracks for each specimen, and then it was gripped and loaded in a uniaxial direction. According to ASTM E399 [26], the fracture toughness ($K_{IC}$) in the opening mode (I) of the DENT specimen can be calculated using equations (1) and (2).

$$K_{IC} = \sigma_c \sqrt{\pi a}\, F\left(a/b\right) \quad (1)$$

$$F\left(a/b\right) = 1.12 + 0.203\left(a/b\right) - 1.197\left(a/b\right)^2 - 1.93\left(a/b\right)^3 \quad (2)$$

Where, $K_{IC}$ is fracture toughness ($MPa.m^{0.5}$), a is the crack length, 2b is the width, and $F\left(a/b\right)$ is a geometric correction factor. Introducing sided cracks with a length of 1mm into the tested specimen deteriorated the mechanical integrity of such films, as shown in Figure 2b. Moreover, the acquired fracture toughness and failure strain show dependency on the applied strain rate. The fracture toughness ($K_{IC}$) increases with the increased applied strain rate. As illustrated in Figure 2c, it accomplished 1.37±0.15, 1.65±0.078, and 1.77±0.008 $MPa.m^{0.5}$ for stain rates of 0.001, 0.01, and 0.1 $min^{-1}$, respectively. This represents a drop of about 6.7% and 22.6% for the samples tested under 0.01 and 0.001 $min^{-1}$, respectively, compared with those tested under 0.1 $min^{-1}$. However, minor changes were observed in the acquired failure strain.

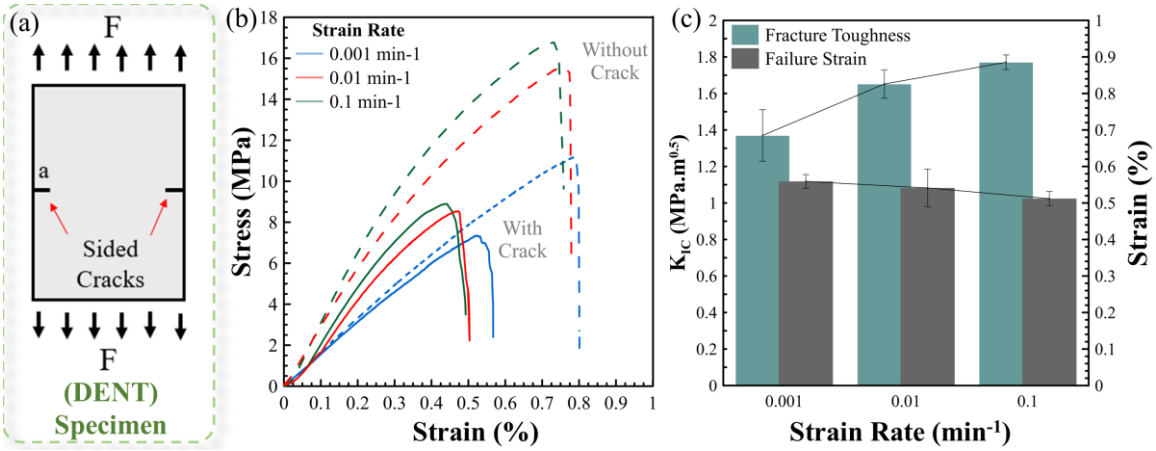


**Figure 2.** (a) Geometry of double edge notched tension (DENT) specimen. (b) Stress-strain curves of $Ti_3C_2T_x$ MXene films with and without cracks. (c) Bar chart of the obtained fracture toughness and failure strain of $Ti_3C_2T_x$ MXene films.

*3.3. Other Properties*

Among the known 2D materials, $Ti_3C_2T_x$ MXene films are recognized as highly electrically conductive materials that originate from their metallic conductivity [19]. As-prepared 18µm thick $Ti_3C_2T_x$ MXene film exhibits electrical conductivity of 2300 $S.cm^{-1}$. This remarkable electrical conductivity is due to the significant electron density of states near the Fermi level [$N(E_f)$] [27]. Additionally, it arises from the well-compacted structure that is composed of overlapped and aligned flakes with large lateral sizes, as shown in Figure 1g. This electrical conductivity endows the films with considerable EMI shielding properties. The various properties of $Ti_3C_2T_x$ MXene films including electrical conductivity and total EMI SE are presented in Figure 3c.

$$SE_T = SE_A + SE_R \quad (3)$$

$$SE_R(dB) = -10\ log\ (1 - R) \quad (4)$$

$$SE_R(dB) = -10\ log\left(\frac{T}{1-R}\right) \quad (5)$$

The total EMI shielding effectiveness ($SE_T$) is expressed in equation (3) [28]. The reflection shielding effectiveness ($SE_R$) and absorption shielding effectiveness ($SE_A$) can be calculated using equations (4) and (5), respectively, where R and T represent the power coefficient of reflectivity, and transmissivity, respectively, that can be calculated based on the measured scattering (S) parameters ($S_{11}$, $S_{21}$), as shown in Figure 3a. Figure 3b illustrates the EMI shielding performance of the $Ti_3C_2T_x$ MXene films in the range of 8.2–12.4 GHz. It is obvious that the total EMI shielding effectiveness ($SE_T$) accomplished a remarkable performance of over 44±2.7 dB. Indeed, EMI shielding results from absorption ($SE_A$=22.2±2.65 dB) is greater than that achieved by reflection ($SE_A$=21.7±2.1 dB). This remarkable absorption performance originates from multiple internal reflections. However, the power coefficient of reflectivity (R) reached 0.99±0.003 compared to 0.01±0.002 for the power coefficient of absorptivity (A). Moreover, the EMI shielding performance exhibits a considerable sensitivity toward the frequency.

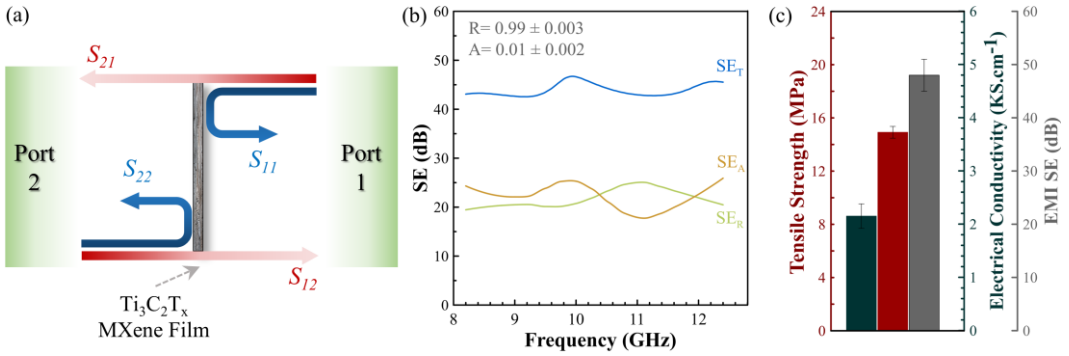


**Figure 3.** (a) EMI shielding setup and the scattering parameters. (b) EMI SE in the X-band frequency range (8.2–12.4 GHz). (c) Bar chart of the acquired mechanical, electrical properties, and the total EMI shielding performance of $Ti_3C_2T_x$ MXene film.

## 4. Conclusion

Thin films constructed from $Ti_3C_2T_x$ MXene have a compacted structure of overlapped nanoflakes. This thin structure can exhibit outstanding properties depending on the interlayer characteristics between the constituent flakes. Therefore, they represent a typical candidate for numerous applications. In this work, the fracture properties of such films in the presence of small-sided cracks were investigated. Additionally, the mechanical properties, electrical conductivity, and electromagnetic interference (EMI) shielding were studied. The results show that small-sided cracks deteriorate the mechanical integrity of the $Ti_3C_2T_x$ MXene films. Furthermore, the deformation of the MXene films exhibits a dependency on the applied strain rate. The higher the strain rate, the higher the tensile strength and fracture toughness ($K_{IC}$). This behavior is due to the interlayer characteristics and the relative sliding between the adjacent nanoflakes.

## Acknowledgment

The authors acknowledge the support granted by the Research & Innovation Center for Graphene and 2D Materials (RIC-2D) of Khalifa University under Award No. DP4-8434000508.

## References

[1] Wang G, Hou H, Yan Y, Jagatramka R, Shirsalimian A, Wang Y, Li B, Daly M and Cao C 2023 Recent advances in the mechanics of 2D materials *Int. J. Extrem. Manuf.* **5** 32002

[2] Rong C, Su T, Li Z, Chu T, Zhu M, Yan Y, Zhang B and Xuan F-Z 2024 Elastic properties and tensile strength of 2D $Ti_3C_2T_x$ MXene monolayers *Nat. Commun.* **15** 1566

[3] Lee C, Wei X, Kysar J W and Hone J 2008 Measurement of the elastic properties and intrinsic strength of monolayer graphene *Science.* **321** 385–8

[4] Androulidakis C, Zhang K, Robertson M and Tawfick S 2018 Tailoring the mechanical properties of 2D materials and heterostructures *2D Mater.* **5** 32005

[5] Shanmugam V, Mensah R A, Babu K, Gawusu S, Chanda A, Tu Y, Neisiany R E, Försth M, Sas G and Das O 2022 A Review of the synthesis, properties, and applications of 2D materials *Part. Part. Syst. Charact.* **39** 2200031

[6] Khalid M Y, Kamal A, Otabil A, Mamoun O and Liao K 2023 Graphene/epoxy nanocomposites for improved fracture toughness: A focused review on toughening mechanism *Chem. Eng. J. Adv.* **16** 100537

[7] Alkrunz M, Shajahan S, Elkaffas R, Schiffer A, Zheng L, Liao K, Khan M Y, Anjum D, Zweiri Y and Abdul Samad Y 2024 Fabrication and characterization of rippled graphene/LDPE composites with enhanced hydrogen barrier properties *Int. J. Hydrogen Energy* **85** 794–803

[8] Ji D, Li B, Zhang D, Raj B T, Rezeq M, Cantwell W and Zheng L 2025 A multifunctional MXene/PVA Hydrogel as a continuous ionic thermoelectric generator and a strain/temperature

Sensor *Small* **21** 2407529
[9] Peng L, Xu Z, Liu Z, Guo Y, Li P and Gao C 2017 Ultrahigh thermal conductive yet superflexible graphene films *Adv. Mater.* **29** 1700589
[10] Dikin D A, Stankovich S, Zimney E J, Piner R D, Dommett G H B, Evmenenko G, Nguyen S T and Ruoff R S 2007 Preparation and characterization of graphene oxide paper *Nature* **448** 457–60
[11] Mohammadlou B S and Gogotsi Y 2025 Assembly of ultrastrong functional MXene films *Sci. China Chem.*
[12] Luo S, Patole S, Anwer S, Li B, Delclos T, Gogotsi O, Zahorodna V, Balitskyi V and Liao K 2020 Tensile behaviors of $Ti_3C_2T_x$ (MXene) films *Nanotechnology* **31** 395704
[13] Kamal A, Li B, Solayman A, Luo S, Kinloch I, Zheng L and Liao K 2025 Mechanical properties of two-dimensional material-based thin films: a comprehensive review *Nanoscale Horizons*
[14] Kamal A, Li B, Luo S, Kinloch I, Zheng L and Liao K 2025 Engineering the mechanical properties of $Ti_3C_2T_x$ MXene films via thermal annealing treatment *Nano Mater. Sci.*
[15] Zhang J, Kong N, Uzun S, Levitt A, Seyedin S, Lynch P A, Qin S, Han M, Yang W, Liu J, Wang X, Gogotsi Y and Razal J M 2020 Scalable manufacturing of free-standing, strong $Ti_3C_2T_x$ MXene films with outstanding conductivity *Adv. Mater.* **32** 2001093
[16] Wan S, Li X, Chen Y, Liu N, Wang S, Du Y, Xu Z, Deng X, Dou S, Jiang L, and Cheng Q 2022 Ultrastrong MXene films via the synergy of intercalating small flakes and interfacial bridging **13** 7340
[17] Vinod S, Tiwary C S, Machado L D, Ozden S, Cho J, Shaw P, Vajtai R, Galvão D S and Ajayan P M 2016 Strain rate dependent shear plasticity in graphite oxide *Nano Lett.* **16** 1127–31
[18] Nizam Uddin M, Huang Z-D, Mai Y-W and Kim J-K 2014 Tensile and tearing fracture properties of graphene oxide papers intercalated with carbon nanotubes *Carbon N. Y.* **77** 481–91
[19] Lipatov A, Goad A, Loes M J, Vorobeva N S, Abourahma J, Gogotsi Y and Sinitskii A 2021 High electrical conductivity and breakdown current density of individual monolayer $Ti_3C_2T_x$ MXene flakes *Matter* **4** 1413–27
[20] Verma R, Thakur P, Chauhan A, Jasrotia R and Thakur A 2023 A review on MXene and its' composites for electromagnetic interference (EMI) shielding applications *Carbon N. Y.* **208** 170–90
[21] Shahzad F, Alhabeb M, Hatter C B, Anasori B, Man Hong S, Koo C M and Gogotsi Y 2016 Electromagnetic interference shielding with 2D transition metal carbides (MXenes) *Science (80-. ).* **353** 1137–40
[22] Jia X, Shen B, Zhang L and Zheng W 2020 Waterproof MXene-decorated wood-pulp fabrics for high-efficiency electromagnetic interference shielding and Joule heating *Compos. Part B Eng.* **198** 108250
[23] Li B, Luo S, Anwer S, Chan V and Liao K 2022 Heterogeneous films assembled from $Ti_3C_2T_x$ MXene and porous double-layered carbon nanosheets for high-performance electromagnetic interference shielding *Appl. Surf. Sci.* **599** 153944
[24] Naguib M, Mashtalir O, Carle J, Presser V, Lu J, Hultman L, Gogotsi Y and Barsoum M W 2012 Two-dimensional transition metal carbides *ACS Nano* **6** 1322–31
[25] Liu S, Hu K, Cerruti M and Barthelat F 2020 Ultra-stiff graphene oxide paper prepared by directed-flow vacuum filtration *Carbon N. Y.* **158** 426–34
[26] Mechanics A I C E on F and F S E 07 on F 2013 *Standard Test Method for Linear-elastic Plane-strain Fracture Toughness K [Ic] of Metallic Materials* (ASTM international)
[27] Khazaei M, Arai M, Sasaki T, Chung C-Y, Venkataramanan N S, Estili M, Sakka Y and Kawazoe Y 2013 Novel electronic and magnetic properties of two-dimensional transition metal carbides and nitrides *Adv. Funct. Mater.* **23** 2185–92
[28] Schulz R B, Plantz V C and Brush D R 1988 Shielding theory and practice *IEEE Trans. Electromagn. Compat.* **30** 187–201